Multi-Functional Fe_3O_4-Au Hybrid Nanostructures for Catalytic Studies

A thesis submitted to

Indian Institute of Science Education and Research Pune in partial fulfillment of the

requirement for the BS-MS Dual Degree Program

by

Angela Dilraj Kadlas

Indian Institute of Science Education and Research Pune

Dr. Homi Bhabha Road, Pashan

Pune, India - 411008

April, 2024

Supervisor: Dr. Pramod P. Pillai

Angela Dilraj Kadlas

Certificate

This is to certify that this dissertation entitled ***'Multi-Functional Fe_3O_4-Au Hybrid Nanostructures for Catalytic Studies'*** towards the partial fulfillment of the BS-MS dual degree program at the Indian Institute of Science Education and Research, Pune, represents study/work carried out by **Angela Dilraj Kadlas** at **Indian Institute of Science Education and Research** under the supervision of **Dr. Pramod P. Pillai**, Associate Professor, Department of Chemistry, during the academic year 2023-2024.

Angela Dilraj Kadlas

Dr. Pramod P. Pillai

27 March 2024

Dedicated to

Mummy, Papa, Eureka, Deep, and All Loved Ones

Declaration

I hereby declare that the matter embodied in the report entitled ***'Multi-Functional Fe_3O_4-Au Hybrid Nanostructures for Catalytic Studies'*** are the results of the work carried out by me at the Department of Chemistry, Indian Institute of Science Education and Research, Pune, under the supervision of Dr. Pramod P. Pillai and the same has not been submitted elsewhere for any other degree. Wherever others contribute, every effort is made to indicate this clearly, with due reference to the literature and acknowledgment of collaborative research and discussions.

Angela Dilraj Kadlas

20191202

27 March 2024

Dr. Pramod P. Pillai

Acknowledgment

My graduation stands as an important milestone in my life. My journey would have been incomplete without the presence of a few people who hold a significant role in shaping my academic and personal life. I want to take this opportunity to thank each one of them for their help and presence.

First and foremost, I would like to express my sincere gratitude to my supervisor, **Dr. Pramod P. Pillai**, for his constant support and guidance throughout my tenure in his group. I'll always be grateful for all his advice and suggestions to succeed academically and in life. Because of him and the NanoAlchemy group, I aspire to pursue my career in science, and I'll always be thankful to them.

I want to thank my Thesis Advisory Committee member, **Dr. Nirmalya Ballav**, for his valuable suggestions during my thesis. Also, I would like to thank **Prof. Jayant B. Udgaonkar** (Former Director, IISER Pune), **Prof. Sunil Bhagwat** (Director, IISER Pune), **Prof. Nirmala Ballav** (Chair, Department of Chemistry, IISER Pune) and **Department of Chemistry** for all the academic and research facilities.

Sumit Roy, who was always there for me. No matter what mess I made, he was there for me. I am grateful to have received a mentor like him who taught me how to think and do research. From the bottom of my heart, "Thank you, Sumit Bhaiya, for everything."

The **Nanoalchemy Group**, my *family away from home*. I was fortunate to have found seniors and labmates like them. I learned a lot from everyone. **Kashyap Ji, Pradyut bhaiya, Indro bhaiya, Ankit bhaiya, Vanshika di, Shreya di, Adhra di, Namitha, Sujitha and Mridul** made lab feel like home.

I am thankful to all my professors at IISER Pune since they greatly fostered my interest in science. I sincerely thank **Dr. Angshuman Nag** and **Professor Anirban Hazra** for inculcating my interest in physical chemistry. I would also like to thank **Mr. Santosh Khilare** and **Mr. Prashant Kale** from the physics department, who helped me devise an over-headed stirrer for my experiments.

All my friends have made a massive contribution to making my time at IISER Pune memorable. I have all the fun memories and unfiltered conversations I had with **Shruti, Kumar, Somen, Namitha, Darshini, Daksh, Soham, and Aashay**. I wish I could say goodbye to **Nilesh** because he was an angel. My juniors **Namith, Sampada, Jassi, Bhavik, Ananya, Bhavesh, Pratiksha, and Manish** gave me a fantastic company. I cannot imagine my life at IISER without these wonderful people. Thank you, guys, for being there for me.

I am indebted to **Singh Uncle** and **Singh Aunty**, my first teachers. Their presence is and will always be crucial in my life. I am thankful to my **parents** for supporting and believing me throughout. They have always been my strength during the tough times we had. I am grateful to everyone for their presence in my life.

Table of Contents

Table of Figures

Abstract

Most of the intriguing properties at the nanoscale lie in the complex hybrid state rather than in the individual counterparts. Therefore, there is a need to create hybrid nanostructures that exhibit advanced optoelectronic properties such as better charge extraction, higher mechanical stability, coupling of inherently different sets of functions, etc. These hybrid architectures are beneficial because they allow one to take advantage of both the inherent features of each component separately. In this project, we have synthesized a hybrid nanostructure of Fe_3O_4-Au nanoparticles for using both the plasmonic and magnetic properties in catalytic and photocatalytic studies. The hybrid structure was well-characterized through various spectroscopy and microscopy techniques. For catalytic property of the hybrid Fe_3O_4-Au structure, an AuNP-based model catalytic 4-nitrophenol (PNP) to 4-aminophenol (AMP) reduction reaction was performed. The plasmonic property of AuNPs was also utilized for the photocatalytic ferricyanide reaction. The hybrid structure's magnetic property allowed us to carry out several catalytic cycles without losing any catalytic activity. In short, our work depicts the importance of hybrid nanoarchitecture in catalytic studies.

Introduction

With the continuous increase in energy demand, a need to develop a sustainable and reliable energy source has drawn much attention worldwide. One of the emerging ways is to harvest energy from electromagnetic radiation for energy production and storage, functional chemical transformations, etc. [1-8] Proper materials that can interact with sunlight efficiently and use the enormous energy stored in the sunlight for breaking and forming of various chemical bonds are crucial. Over the past few decades, nanostructures that exhibit optical and electrical activity, stability, and so on have gained immense significance. They show different properties because of the quantum confinement effect and significant surface-to-volume ratio, in contrast to their bulk counterparts. [9] In semiconductor nanoparticles, upon electromagnetic irradiation an electron is excited from its valence band to the conduction band. On the other hand, plasmonic metal nanoparticles (e.g., Au and Ag NPs) are known to have a 'sea of electrons' which, upon visible light irradiation, start to oscillate, and a resonance condition is achieved which is termed as localized surface plasmon resonance (LSPR) when the electromagnetic radiation's frequency aligns with the electrons' oscillation. [18-19] Both these nanostructures are known to have high molar extinction coefficients, due to which they can absorb massive amounts of light and generate large number of high-energy charge carriers that can be used for thermodynamically uphill chemical transformations (e.g., H_2O splitting, N_2 reduction, NO_3^-, CO_2 reduction, etc.). As a result, both metal and semiconductor nanoparticles are well known for their unique light harvesting properties, thereby cementing a special place in catalysis and photocatalysis. [10-15, 18-23]

However, it was observed that the emerging properties could be efficiently harvested from the assembly of particles rather than individual counterparts, for example, Au-TiO_2, Au-Pd, and Au-Rh nanoparticles. This has led to extensive research in enhanced and emerging properties through the design and development of hybrid materials. Such a hybrid structure is also essential because we can utilize different properties in a single system. Such hybrid systems are generally prepared through in-situ synthesis or the self-assembly approaches. [24-25] One of the fascinating combinations is to couple plasmonic and magnetic properties. Magnetic nanoparticles, especially

magnetite (Fe_3O_4) NPs, are being explored for their high magnetic susceptibility and low toxicity, and they are employed in MRI (Magnetic Resonance Imaging), self-assembly, catalysis, etc. [26-27] While LSPR of plasmonic nanoparticles such as AuNPs are investigated for various sensing, photocatalytic, and photothermal applications. [28] Therefore, it is interesting to couple magnetic and plasmonic NPs to realize the inherently absent properties of the individual components in hybrid structures.

In this project, we employ Fe_3O_4-Au hetero nanostructures for catalytic and photocatalytic applications. One of the significant challenges associated with nanoparticle catalysis is the separation of catalysts after the reaction, which also creates obstacles for the easy analysis of the reaction mixture. This challenge can be overcome by installing magnetic nanoparticles in plasmonic nanoparticles. Iron oxide is known to be magnetic, which would ensure a separation under external magnetic field. [26-27] According to literature reports, iron oxide acts as a semiconductor. When present in a heterostructure, they can provide better charge separation, provided they form heterojunction and their energy levels match with the counterpart. [27] In this project, we have synthesized and characterized Fe_3O_4-Au hybrid nanostructures. Further, we explored these hybrid structures for model catalytic 4-nitrophenol reduction and photocatalytic one electron reduction of ferricyanide (details on these catalytic reactions are given in Section 1.1). More importantly, the magnetic properties of Fe_3O_4 NPs in the hybrid was used for the easy separation of the catalyst, which enabled us to perform multiple catalytic cycles without any compromise in the catalytic activity. In short, our work provides a simple, yet effective strategy to achieve recyclability in NP catalysed reactions, while retaining the excellent catalytic activity.

1.1. Gold-Catalyzed Reactions:

1.1a) Passive Catalysis

Metal nanoparticle catalysis is widely studied because it exhibits unusual behavior at the nanoscale compared to its bulk counterparts. Metal nanoparticles are known to participate in chemical transformations passively. They provide their surface to adsorb the substrates to overcome the kinetic barrier, thus facilitating the reaction. A widely used model reaction to inspect the passive participation of nanoparticles is p-nitrophenol (PNP)

to p-aminophenol (AMP/PAP) in the presence of borohydride (BH_4^-) which is the reducing agent. PNP and borohydride ions are adsorbed on the surface of Au nanoparticles, where the Langmuir-Hinshelwood mechanism facilitates electron transfer between the two moieties. Though PNP reduction is a thermodynamically feasible reaction it only progresses in presence of a catalyst. [29-31]

1.1b) Active Catalysis

Plasmonic metal nanoparticles are known to have large number of mobile charge carriers. The free electron cloud oscillates continuously in the external field upon electromagnetic irradiation. [9,28] The charge carriers stay in phase with the external field and internal polarization reaches equilibrium if the driving force frequency is relatively low. (**Fig. 1.1.a**). [28] A resonance condition is achieved at frequencies higher than the driving force. In presence of external electromagnetic field with frequency higher than driving force, the internal polarization is developed as a result of charge oscillation in the nanoparticle lagging behind by a phase of π/2 with respect to the external field. When the system is excited at its resonant frequency, the internal polarization increases rather than cancelling out the driving force. Plasmonic metal nanoparticles exhibit significant charge polarization and an increase in oscillation amplitude when excited at their resonant frequency. This results in plasmonic amplification of the particle's near field. (**Fig. 1.1.b**). This condition is termed localized surface plasmon resonance (LSPR). [28]

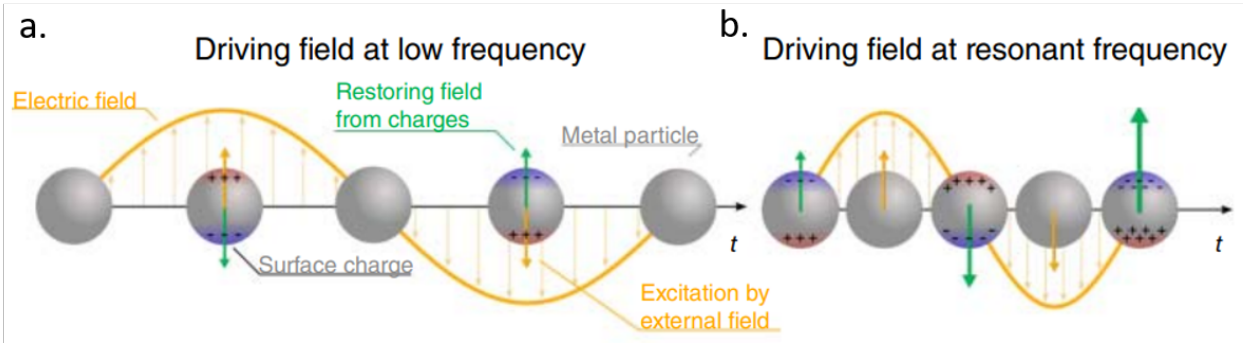

Figure 1.1: Schematic depiction of oscillation of charge carriers in a metal nanoparticle at a) low and b) resonant frequency. Adapted with permission. [28] Copyright 2021, Wiley-VCH.

Localized surface plasmon resonance undergoes Landau damping by dephasing, followed by radiative or nonradiative decay at the femtosecond timescale. [9,28,32]

Radiative decay happens via emitting photons (luminescence or scattering), which is dominant for larger particles (>50 nm), and nonradiative decay occurs by the formation of hot charge carriers, which is dominant for smaller particles. [9] In nonradiative pathways, hot charge carriers are formed in two ways: interband excitation, here electrons transition from low-lying filled d band to the empty sp band above the Fermi energy level (ε_f) in a metal nanoparticle. In intraband excitation, electrons transition from filled sp band to the empty sp band, which is above the Fermi energy level. [28] Following these transitions, non-fermi electronic distribution is created via Landau dampening (within 100 fs), which thermalizes internally by electron-electron, electron-phonon, and phonon-phonon scattering. Ultimately, by dissipating heat, the nanoparticle lattice achieves thermal equilibrium with the surrounding. [32] To employ plasmonic nanoparticles for photocatalytic applications, they should be photoexcited first for the formation of hot charge carriers. Various light-driven chemical reactions are facilitated by the extraction of these hot charge carriers. [33]

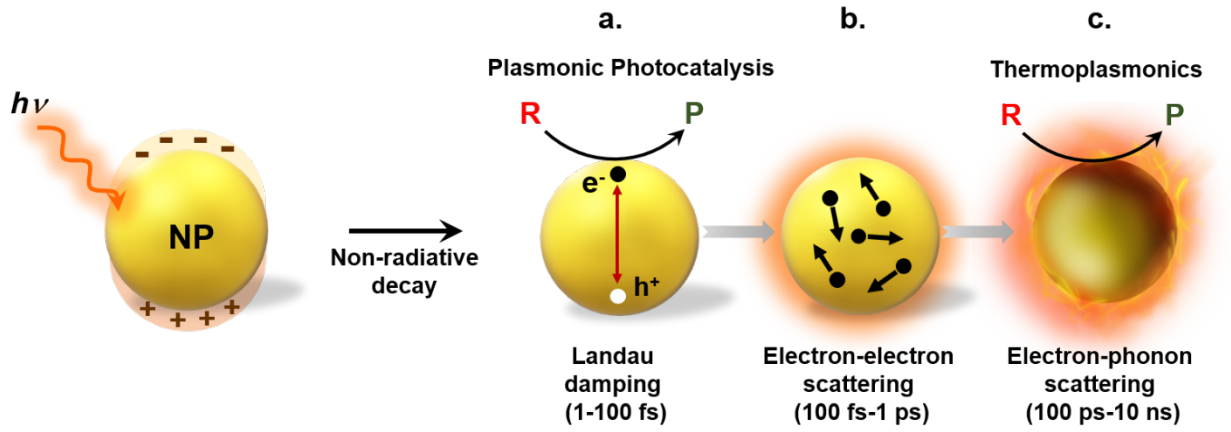

Figure 1.2: Plasmon relaxation dynamics. Because of plasmonic excitation, the local electric fields dissipate the energy in two ways: radiative or nonradiative decay paths. Hot charge carriers and heat are produced via nonradiative decay. (a) At t = 0, plasmon excitation decays non-radiatively to produce a hot charge carrier distribution that takes 1–10 fs to generate before being thermalized by electron–electron scattering, (b) electron–phonon scattering, and (c) phonon–phonon scattering. Ultimately, the energy is released into the surrounding as heat.

Materials and Methods

2.1. Materials and Reagents

Iron (III) chloride hexahydrate ($FeCl_3 \cdot 6H_2O$, 97%, SRI), ethylene glycol (98%, Avra), polyvinylpyrrolidone (PVP, average MW~55,00), sodium acetate (99%, Rankem), chloroauric acid trihydrate ($HAuCl_4 \cdot 3H_2O$, ≥99.9%, Sigma-Aldrich), 4-nitrophenol (≥99%, Sigma-Aldrich), sodium citrate tribasic dihydrate (≥99.0%, Sigma-Aldrich), sodium borohydride (≥99%, Sigma-Aldrich), ethanol absolute (>99%, Alsucrose corporation), potassium Hexacyanoferrate (≥99%, Sigma-Aldrich), Milli-Q water.

2.2. Synthesis

2.2a) Synthesis of multicore Fe_3O_4 nanoparticles

The Fe_3O_4 NPs were synthesized by modifying a previous report. [34] In a typical experiment, $FeCl_3 \cdot 6H_2O$ (114 mg) was dissolved in ethylene glycol (72.6 mL) in a round bottom flask followed by PVP (400 mg) once it reached 60°C under vigorous stirring conditions. Then, sodium acetate (853 mg) was added to the solution. The reaction mixture was heated in an oven for four hours at 200°C in a Teflon autoclave. The mixture was gradually cooled over a 12-hour period. The final mixture was twice centrifuged (6500 rpm, 4 min) with ethanol and once with Milli-Q water. Finally, the nanoparticles were dispersed in 75 mL Milli-Q water.

2.2b) Synthesis of Au nanoparticles

The Au NPs were synthesized according to a modified literature report. [35] In a typical experiment, 2.7 mL $HAuCl_4 \cdot 3H_2O$ (25 mM) was added to 270 mL Milli-Q water and heated to 95°C. Subsequently, 8.1 mL sodium citrate (38.7 mM) was added. After 10 min, the nanoparticles were stored in the fridge until further use.

2.2c) Synthesis of hybrid Fe_3O_4-Au nanoparticles

The Fe_3O_4 NPs were synthesized following a modified previous report. [34] 10 mL of Fe_3O_4 nanoparticles were separated using a magnet; then, the solution was removed, and the previously prepared 21 mL of citrate capped Au NP were added. The solution was sonicated for three hours and stirred in a vortex mixer for two hours. The product was dispersed into 3 mL of milli-Q water after being repeatedly washed with a magnet.

2.3. Characterization

2.3a) Transmission electron microscopy (TEM)

On the Jeol JEM2200FS (200 kV) apparatus, the Transmission Electron Microscopic (TEM) investigations were conducted. After letting the sample rest undisturbed for about ten minutes, diluted AuNP solutions were drop-cast onto 400 mesh carbon-coated copper grids (Ted Pella Inc.). Following the samples' complete vacuum drying, imaging was done.

2.3b) X-ray photoelectron spectroscopy (XPS)

Thermo Scientific K-Alpha fully integrated, monochromated small-spot X-ray photoelectron spectrometer (XPS) instrument was used to perform X-ray photoelectron spectroscopy. The Fe_3O_4-Au nanoparticle sample was dried completely by lyophilization before the spectra were recorded.

2.4. Catalytic Reduction

UV-vis absorption spectroscopy (SHIMADZU UV-3600 plus UV-VIS-NIR spectrophotometer) was used to track the kinetics of all Fe_3O_4-Au NP mediated reduction reactions. The UV-vis absorption spectra were obtained at one-minute intervals in a 3 mL cuvette (path length = 1 cm). In order to conduct time-dependent kinetic studies, the reactant's absorbance at its λ_{max} was tracked over time. All tests were performed at room temperature. The molar extinction coefficient for Au nanoparticles was taken to be 5.4 x 10^7 $M^{-1}cm^{-1}$. [36-37]

2.4a) Catalytic reduction of p-nitrophenol (PNP)

The standard Au NP-mediated catalytic reduction of p-nitrophenol (PNP) by BH_4^- ions involved mixing in a cuvette 300 µL of 0.1 M $NaBH_4$, 100 µL of Fe_3O_4-Au NP solution, and 6 µL of 50 mM PNP and milli-Q water. UV-vis absorption spectroscopy was used to monitor the progress of the reaction. The absorbance at ~400 nm (nitrophenolate ion) decreases gradually with time with increase in absorbance at ~300 nm (aminophenolate ion), confirming the reduction process.

2.5. Photocatalytic Reduction

UV-vis absorption spectroscopy (SHIMADZU UV-3600 plus UV-VIS-NIR spectrophotometer) was used to track the kinetics of all Fe_3O_4-Au NP mediated photocatalytic reduction reactions. The reaction mixture's UV-vis absorption spectra were obtained at fifteen-minute intervals in a 3 mL cuvette (path length = 1 cm). In order to conduct time-dependent kinetic studies, the reactant's absorbance at its λ_{max} was tracked over time. All tests were performed at room temperature.

2.5.a) Photocatalytic reduction of Ferricyanide

The photocatalytic activity of Fe_3O_4-Au NPs was investigated for ferricyanide reduction to ferrocyanide. At room temperature, the reaction was carried out in a 3 mL quartz cuvette, illuminated by two 3W Blue LEDs (465nm, ~60mW/cm²). A mixture of 880 µL 5M EtOH (hole scavenger), 250 µM potassium ferricyanide, and 400 µL Fe_3O_4-Au NPs was purged with Ar for 15 minutes before irradiation. Ferricyanide reduction was monitored over 2 hours by measuring the change in the absorbance at 420 nm, corresponding to ferricyanide.

2.6. Determination of Conversion, Reaction rate (k') and Rate constant (k)

Assuming that the conversion of reactant to product was pseudo-first-order with respect to PNP concentration, the rate of catalytic reduction reaction was calculated. In the case of PNP reduction reaction, the decrease in the concentration (conversion at time t) of p-nitrophenolate at 400 nm was calculated using Beer-Lambert law, where 18300 $M^{-1}cm^{-1}$ was used as the molar extinction coefficient of p-nitrophenolate [38] i.e.,

$$Conversion\ (t) = -\frac{(A_{400\,nm}\ (t) - A_{400\,nm}\ (t=0)}{18300}$$

The rate of catalytic reduction reaction was determined by assuming the conversion of reactant to the product was first-order in the ferricyanide reduction reaction. In the case of the ferricyanide reduction reaction, the decrease in the concentration (conversion at time t) of ferricyanide at 420 nm was calculated using Beer-Lambert law, where 1050 $M^{-1}cm^{-1}$ was used as the molar extinction coefficient of ferricyanide [39] i.e.,

$$Conversion\ (t) = -\frac{(A_{420\,nm}\ (t) - A_{420\,nm}\ (t=0)}{1050}$$

The reaction rate was determined by fitting the conversion vs. time (t) plot with a function given below

$$c = c_0\,(1 - e^{-kt})$$

Here, c_0 stands for initial concentration of PNP and ferricyanide in PNP and ferricyanide reduction reactions respectively and k stands for the rate constant of the reaction. Rate of reaction is represented below

$$\frac{dc}{dt} = c_0.k.e^{-kt}$$

Reaction rate at t = 0 is given as

$$k' = \frac{dc}{dt}(t=0) = c_0.k$$

The following equation determined the rate constant, k

$$k = \frac{k'}{c_0}$$

Where c_0 was taken as 10^{-4} M in the case of PNP and corresponding of ferricyanide in ferricyanide reduction.

2.7. Calculation of conversion yield (%)

The conversion yield was calculated by monitoring the decrease in ferricyanide absorbance at ~420 nm.

2.7a) External quantum yield calculation (φ_{EQY})

The external quantum yield (φ_{EQY}) was calculated using the following equation

$$\varphi_{EQY} = \frac{molecules\ of\ product\ formed}{number\ of\ incident\ photons\ per\ second}\ x\ 100$$

$$\varphi_{EQY} = \frac{moles\ of\ product\ formed\ x\ N_A}{\frac{E\lambda t}{hc}}\ x\ 100$$

Here, N_A is Avogadro number, E is excitation energy, λ is wavelength of the excitation source, t is total time of irradiation in seconds, h is Plank's constant and c is speed of light.

The moles of product formed are calculated as follows:

$$moles\ of\ product\ formed = concentration\ x\ volume$$

$$moles\ of\ product\ formed = \frac{Absorbance\ of\ product\ (at\ 420\ nm)}{\varepsilon l} x\ 3\ x\ 10^{-3}\ L$$

$$moles\ of\ product\ formed = \frac{0.248}{1050} x\ 3\ x\ 10^{-3}\ L$$

$$moles\ of\ product\ formed = \ 7.08\ x\ 10^{-7}\ moles$$

The incident power is $35\ mWcm^{-2}$ and area of cuvette is $4\ cm^2$. So, the excitation energy is:

$$Excitation\ energy = Incident\ power\ x\ Area\ of\ cuvette$$

$$Excitation\ energy = 35\ mWcm^{-2}\ x\ 4\ cm^2$$

$$Excitation\ energy = 140\ mW\ or\ 140\ mJs^{-1}$$

The number of incident photons per second is:

$$\frac{E\lambda t}{hc} = \frac{0.140\ Js^{-1}\ x\ 465\ nm\ x\ 7200\ s}{6.626\ x\ 10^{-34} Js^{-1}\ x\ 3\ x\ 10^8\ ms^{-1}} = 2.36\ x\ 10^{21}$$

Finally, substituting the values of moles of product formed and number of incident photons per second

$$\varphi_{EQY} = \frac{7.08\ x\ 10^{-7}\ x\ 6.023\ x\ 10^{23}}{2.36\ x\ 10^{21}}\ x\ 100 = 0.018$$

Results and Discussion

A hybrid of plasmonic gold and magnetic iron oxide nanoparticles gives room to study a variety of gold-catalyzed and photocatalyzed reactions, where the hybrid nanoparticles can be recovered after every reaction due to their magnetic activity and can be recycled, ensuring efficient repeated use of the material. The recyclability of the hybrid nanostructures was examined in a model 4-nitrophenol reduction reaction and model $1e^-$ ferricyanide reduction reaction. The 4-nitrophenol reaction proceeded by adsorption of substrates (BH_4^- ions and PNP) on the surface of Au NPs, which helped to overcome the kinetic barrier of the reaction. Model $1e^-$ ferricyanide reduction reaction proceeds by forming hot charge carriers in Au NPs upon light irradiation. The hot electrons are efficiently extracted for reduction reaction and hot holes for oxidation reaction.

3.1. Synthesis and characterization of Fe_3O_4-Au nanoparticles

Multicore Fe_3O_4 nanoparticles were synthesized through a modified polyol-mediated solvothermal synthesis. [34] In a typical reaction mixture, ferric chloride hexahydrate was dissolved in ethylene glycol (a short-chain polyol that allows clustering for multicore particles), followed by the addition of PVP (capping agent) and sodium acetate (helps in the hydrolysis of Fe^{3+} ions). [34, 40-41]

In accordance with previous literature reports, citrate capped AuNPs (11.5 ± 0.5 nm) were synthesized and adsorbed onto these iron oxide nanoparticles. **Scheme 3.1** provides a schematic depiction of the synthesis process**.** Absorption spectra of Fe_3O_4 and hybrid Fe_3O_4-Au nanoparticles are shown in **Figure 3.1.a.**

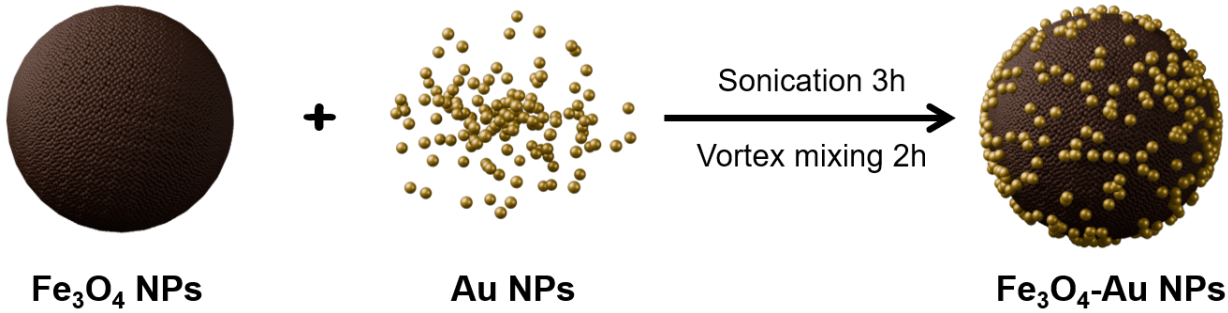

Scheme 3.1: Schematic representation of iron oxide-gold hybrid nanoparticles synthesis.

The synthesized PVP-capped Fe_3O_4 nanoparticles were characterized with diffuse reflectance spectroscopy (DRS) and transmission electron microscopy (TEM). Absorption spectra of Fe_3O_4 nanoparticles were recorded (**Figure 3.1.a**). TEM images confirmed that these multicore nanoparticles were formed from clustering ~5 nm Fe_3O_4 nanoparticles (**Figure 3.1.c**). UV-Vis absorption and transmission electron microscopy characterized the synthesized citrate-capped Au nanoparticles. These nanoparticles exhibited their characteristic red wine color with LSPR peak at ~518 nm (**Figure 3.1.b**), with an estimated size of ~10 nm (**Figure 3.1.d**).

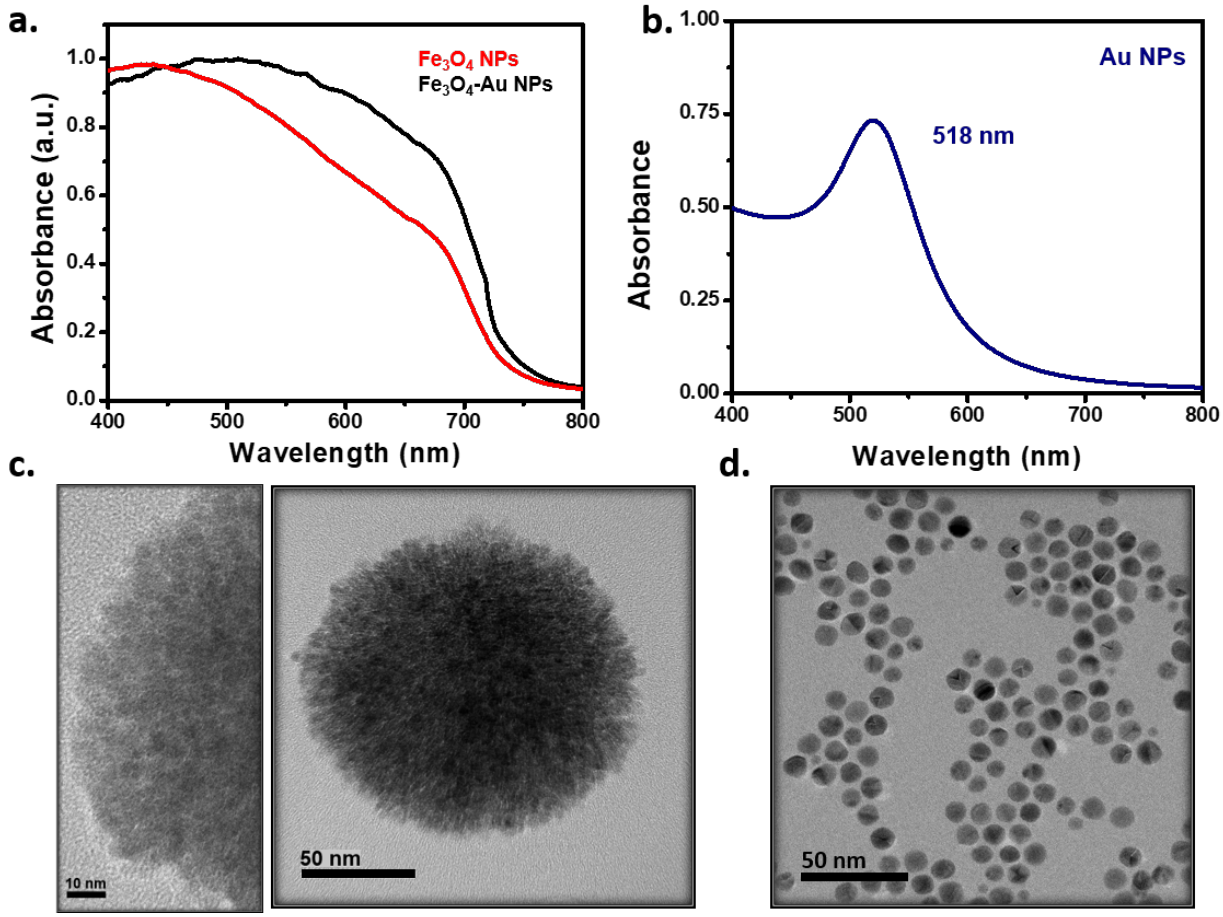

Figure 3.1: Characterization of Fe_3O_4 and Au nanostructures. (a) absorption spectra (DRS) of Fe_3O_4 (black) and Fe_3O_4-Au (red) nanostructures (b) UV-Vis absorption spectra of citrate-capped Au NPs. A representative TEM image of (c) multicore iron oxide nanoparticles formed of ~5 nm Fe_3O_4 nanoparticles and (d) Au nanoparticles.

The morphology and chemical composition of hybrid Fe_3O_4-Au nanoparticles were well characterized through TEM and X-ray photoelectron spectroscopy (XPS). The absorption spectra of hybrid Fe_3O_4-Au nanoparticles were recorded (**Figure 3.1.a**). TEM images confirmed the adsorption of Au nanoparticles onto Fe_3O_4 nanoparticles (**Figure 3.2.a**). Ultimately, structural characterization of Fe_3O_4-Au nanoparticles, XPS investigations were performed. [42] All significant elements namely Fe, Au, C, and O were present in the heterostructures, according to XPS survey spectra. (**Figure 3.2.b**). The Au 4f area has two peaks in the XPS spectra for Au, and they are attributed to the core-energy levels Au $4f_{5/2}$ and Au $4f_{7/2}$. (**Figure 3.2.c**). Similarly, Fe_3O_4 nanoparticles showed two peaks for Fe^{2+} ($2p_{3/2}$ and $2p_{1/2}$) and two peaks for Fe^{3+} ($2p_{3/2}$ and $2p_{1/2}$) along with their satellite peaks (**Figure 3.2.d**). The catalytic and photocatalytic characteristics of AuNP-based hybrid systems were examined after their structural composition and morphology were confirmed for model 4-nitrophenol reduction and model one electron ferricyanide reduction. After purification, the hybrid structures were magnetically separated with a neodymium magnet within a minute (**Figure 3.2.e**).

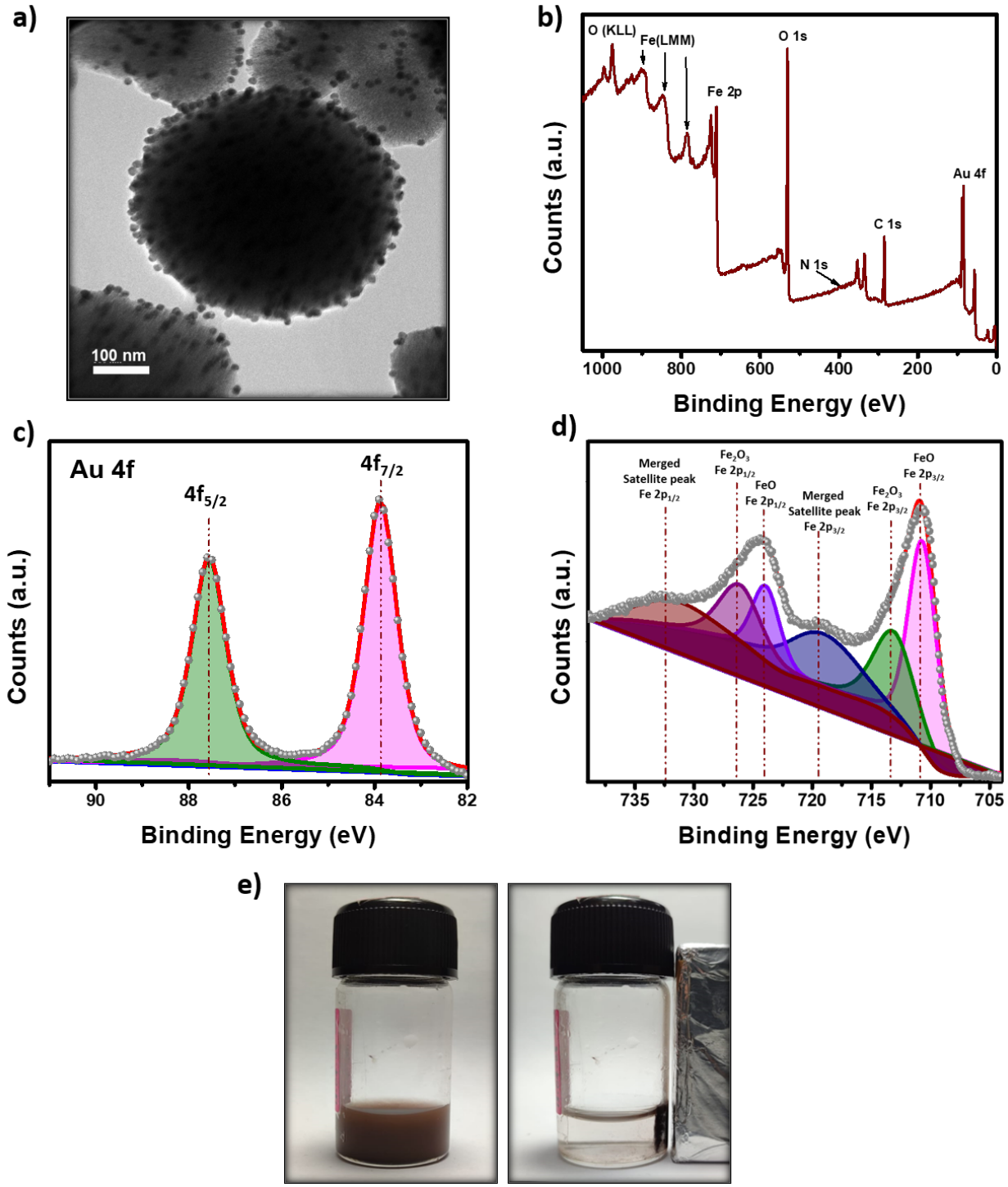

Figure 3.2. Characterization of hybrid Fe_3O_4-Au nanostructures. (a) A TEM image of Au NPs adsorbed on Fe_3O_4 NPs. (b) All significant elements present in the heterostructures, according to XPS survey spectra. XPS spectra of (c) Au 4f core-level and (d) Fe 2p core-level, confirming the presence of both Fe^{2+} and Fe^{3+} oxidation states in Fe_3O_4-Au nanostructures. (e) Optical images of before and after magnetic separation within a minute.

3.2. Catalytic reduction of p-nitrophenol

We employed Fe_3O_4-Au nanostructures to catalyze p-nitrophenol (PNP) to p-aminophenol (AMP) reduction reaction. The negatively charged substrates (BH_4^- and 4-nitrophenolate ions) get adsorbed onto the Au surface, catalyzing the reaction via the Langmuir-Hinshelwood mechanism (**Figure 3.3**). [29-31] Borohydride ions react with the surface of metal nanoparticles and transfer hydride ions onto it. Simultaneously, nitrophenolate ions also get adsorbed on the nanoparticle's surface, and the electron transfer happens between nitrophenolate ion and the surface adsorbed hydride ions followed by dissociation of 4-aminophenol from the metal surface.

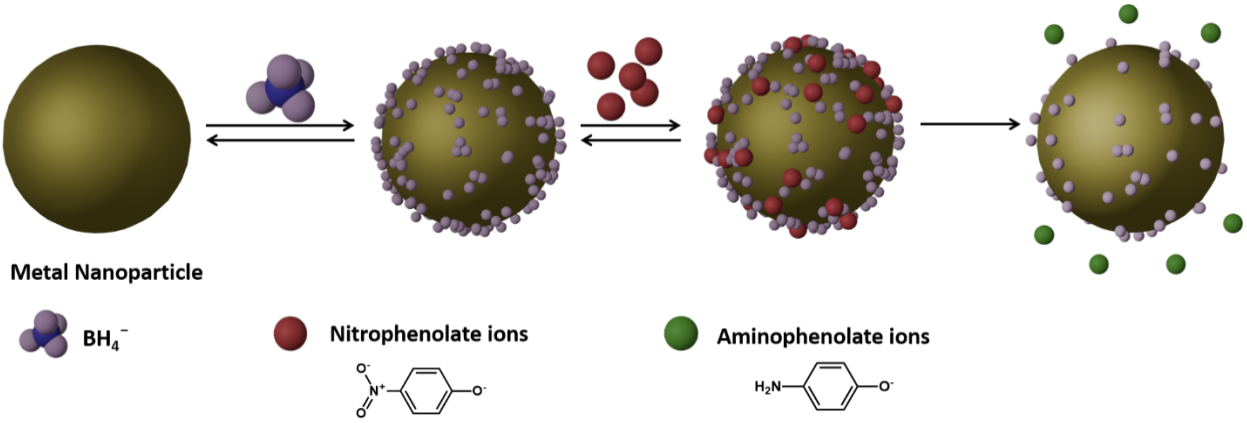

Figure 3.3: Schematic representation of Langmuir-Hinshelwood electron transfer mechanism on the surface of metal nanoparticles. Adapted with permission. [31] Copyright 2022, The Royal Society of Chemistry.

UV-Vis absorption spectroscopy was used to monitor the progress of the reaction. The absorbance at ~400 nm for nitrophenolate ion decreased with time and increased at ~300 nm, corresponding to aminophenol, confirming the reduction process. [29] Because of the presence of excess amounts of BH_4^- over PNP, the reaction kinetics follows pseudo-first-order kinetics, and based on the conversion vs. time plot, the reaction's rate constant (k) was calculated to be ~0.35 min^{-1}. [29,38] The heterogeneous aspect of the catalyst was demonstrated through the easy separation of the catalyst in the presence of

an external magnet, which enabled us to perform recyclability experiments. Interestingly, we obtained five cycles without a significant decrease in the % conversion yield.

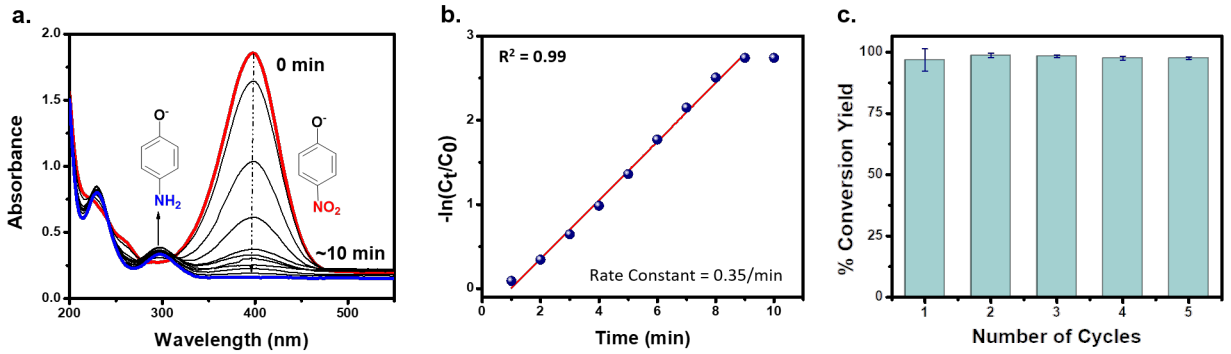

Figure 3.4. Recyclable catalytic reduction of PNP over Fe_3O_4-Au NPs. (a) UV-vis absorption changes of nitrophenolate ion in the presence of BH_4^- and Fe_3O_4-Au nanoparticles. A decrease in the absorption of PNP ion at ~400 nm and the appearance of a new band ~300 nm corresponding to PNA was observed. (b) A pseudo-first-order analysis plot by tracking the PNP absorption changes at 400 nm. (c) The retention of the catalytic properties of Fe_3O_4-Au NPs for five cycles.

3.1 a) Temperature-dependent catalytic study

Next, detailed temperature-dependent kinetic studies were performed to deduce the activation energy of the reaction in the presence of the hybrid structures. The kinetics of the reaction at different temperatures was monitored at 400 nm, which decreased over time, confirming the reduction of PNP (**Figure 3.5.a**). Following the Arrhenius equation, the reaction rate was faster at higher and slower at lower temperatures. Reactions at lower temperatures were associated with longer induction time, which justifies the slower rate. The apparent activation energy for the PNP reduction reaction was estimated to be ~45 kJ/mol from ln k versus 1/T plot (**Figure 3.5.b**).

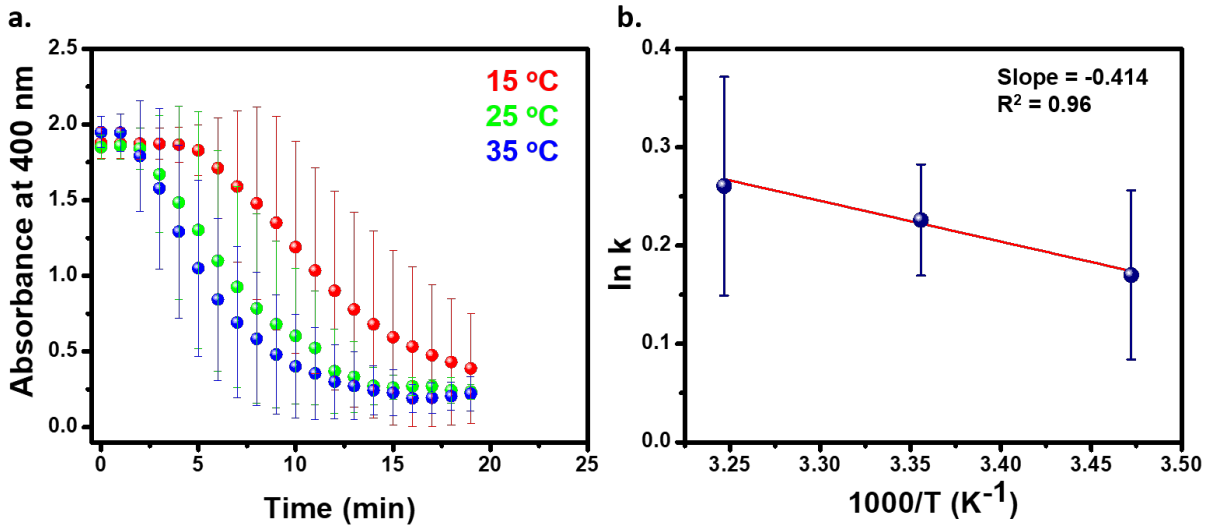

Figure 3.5. Temperature-dependent catalytic study. (a)Temperature-dependent kinetics was monitored at 400 nm at 15°C (red), 25°C (green), and 35°C (blue), respectively. (b) The PNP reduction by BH_4^- plot of ln k versus 1/T in the presence of hybrid Fe_3O_4-Au NPs.

3.3. Photocatalytic reduction of ferricyanide

The photocatalytic activity of Fe_3O_4-Au NPs was investigated for the model ferricyanide to ferrocyanide reduction reaction. In a typical reaction mixture, ferricyanide, ethanol (hole scavenger), and Fe_3O_4-Au were irradiated by two blue (250 mW) LEDs. The photoexcitation of gold nanoparticles leads to the formation of hot charge carriers, which were transferred to the acceptors (ferricyanide and ethanol) to carry out the reduction and oxidation reactions, respectively. [39,43] On the Au NP, an excess electron build-up results from hole scavenging. Au NP develops a substantial steady-state excess of electrons during continuous LSPR activation. Due to this, the quasi-Fermi level rises compared to the Fermi level of Au nanoparticles in the dark. The apparent activation barrier of the reduction from Fe^{3+} to Fe^{2+} is lower than in the dark because of an increase in the chemical potential of the electrons supplied by the photo-charged Au NP relative to the unexcited NP. This decrease in the fermi energy level is due to the light excitation at LSPR. [45]

UV-Vis absorption spectroscopy was used to monitor the progress of the reaction. The absorbance at ~420 nm corresponds to ferricyanide decrease with time along with a gradual increase at ~240 nm, corresponding to ferrocyanide, confirming the reduction

process (**Figure 3.6.a**). The reaction kinetics follows first-order kinetics, and based on the conversion vs. time plot, the reaction's rate constant (k) was calculated to be ~ 0.008 min^{-1} from (**Figure 3.6.b**). The heterogeneous aspect of the catalyst was demonstrated through the easy separation of the catalyst in the presence of an external magnet, which enabled us to perform recyclability experiments. Interestingly, we obtained five cycles without significantly decreasing the % conversion yield (**Figure 3.6.c**).

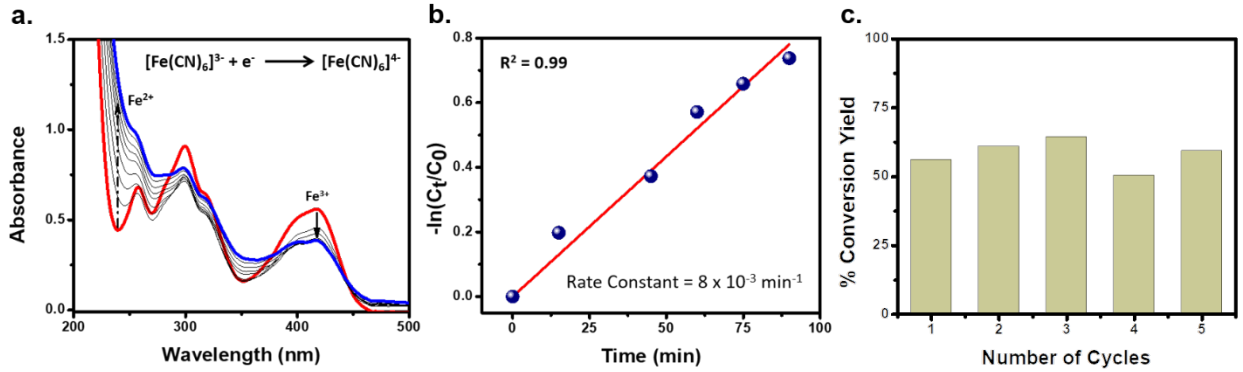

Figure 3.6. Recyclable photocatalytic reduction of ferricyanide by Fe_3O_4-Au NPs. (a) Spectral changes in the absorption of ferricyanide ions in the presence of Fe_3O_4-Au NPs. A gradual decrease in the absorption of ferricyanide ion at ~420 nm, along with the appearance of a new band ~240 nm corresponding to ferrocyanide ion, was observed. (b) A first-order analysis plot by tracking the ferricyanide absorption changes at 420 nm. (c) The retention of the catalytic properties of Fe_3O_4-Au NPs for five cycles.

Conclusion

Our study reveals a set of properties in a single hybrid system. We could successfully integrate fully functional magnetic and plasmonic properties in a hybrid nanoparticle system. We chose magnetic Fe_3O_4 and plasmonic Au nanoparticles in our hybrid system. The well-defined morphology of Fe_3O_4-Au hybrid structures was confirmed by TEM imaging, and the chemical composition was confirmed by XPS studies. The catalytic activity of AuNP in the heterostructures was confirmed by model 4-nitrophenol reduction. Further, model one electron photocatalytic reduction of ferricyanide ensured the hybrid structure retained the plasmonic property. The magnetic property of Fe_3O_4 NP in the heterostructure helped us perform recyclability with Au-catalyzed reactions, further confirming the hybrid structure's superiority.

Future Direction

The hybrid structure will be explored for essential and challenging reactions such as N_2 reduction reaction (NRR), $NO_2^-$and NO_3^- to NH_4^+ production, and CO_2 reduction into valuable fuels. The iron oxide part is expected to adsorb N_2, NO_3^-, and NO_2^- molecules, and plasmonically active gold nanoparticles will optically activate the adsorbed molecules to transform into NH_3. These hybrid nanostructures will also be used for biomolecule sensing and preparing photoelectric cells.

Reference

1. Kamat, P. V. Photophysical, Photochemical and Photocatalytic Aspects of Metal Nanoparticles. *J. Phys. Chem. B* **2002**, *2*, 7729−7744
2. He, Y.; Wang, D. Toward Practical Solar Hydrogen Production. *Chem.* **2018**, *4*, 405– 408
3. Yang, X.; Wang, D. Photocatalysis: from fundamental principles to materials and applications. *ACS Applied Energy Materials* **2018**, *1*, 6657– 6693
4. Aslam, U.; Rao, V. G.; Chavez, S.; Linic, S. Catalytic Conversion of Solar to Chemical Energy on Plasmonic Metal Nanostructures. *Nat. Catal.* **2018**, *1*, 656– 665
5. Gellé, A.; Jin, T.; de la Garza, L.; Price, G. D.; Besteiro, L. V.; Moores, A. Applications of Plasmon-Enhanced Nanocatalysis to Organic Transformations. *Chem. Rev.* **2020**, *120*, 986– 1041
6. Listorti, A.; Durrant, J.; Barber, Solar to fuel. J. *Nat. Mater.* **2009**, *8*, 929
7. Chakraborty, I. N.; Roy, S.; Devatha, G.; Rao, A.; Pillai, P. P. InP/ZnS Quantum Dots as Efficient Visible-Light Photocatalysts for Redox and Carbon-Carbon Coupling Reactions. *Chem. Mater.* **2019**, *31*, 2258– 2262
8. Zhan, C.; Moskovits, M.; Tian, Z. Q. Recent Progress and Prospects in Plasmon-Mediated Chemical Reaction. *Matter* **2020**, *3*, 42– 56
9. Jain, V.; Kashyap, R. K.; Pillai, P. P. Plasmonic Photocatalysis: Activating Chemical Bonds through Light and Plasmon. *Adv. Opt. Mater.* **2022**, *10*, 2200463
10. Mubeen, S.; Lee, J.; Singh, N.; Krämer, S.; Stucky, G. D.; Moskovits, M. An autonomous photosynthetic device in which all charge carriers derive from surface plasmons. *Nat. Nanotechnol.* **2013**, *8*, 247.
11. Verma, R.; Belgamwar, R.; Polshettiwar, V. Plasmonic Photocatalysis for CO_2 Conversion to Chemicals and Fuels. *ACS Materials Letters* **2021**, *3*, 574– 598
12. Medford, A. J.; Hatzell, M. C. Photon-driven nitrogen fixation: current progress, thermodynamic considerations, and future outlook. *ACS Catal.* **2017**, *7*, 2624

13. Minteer, S. D.; Christopher, P.; Linic, S. Recent Developments in Nitrogen Reduction Catalysts: A Virtual Issue. *ACS Energy Lett.* **2019**, *4*, 163– 166
14. Tachibana, Y.; Vayssieres, L.; Durrant, J. R. Artificial Photosynthesis for Solar Water-Splitting. *Nat. Photonics* **2012**, *6*, 511– 518
15. Liu, C.; Dasgupta, N. P.; Yang, P. Semiconductor Nanowires for Artificial Photosynthesis. *Chem. Mater*. **2014**, *26*, 415– 422
16. Roy, S. Photocatalytic Materials for Reduction of Nitroarenes and Nitrates. *J. Phys. Chem. C* **2020**, *124*, 28345– 28358
17. Lakowicz, J. R. *Principles of Fluorescence Spectroscopy*, 3rd ed.; Springer: New York, **1999**.
18. Jain, P. K.; Huang, X. H.; El-Sayed, I. H.; El-Sayed, M. A. Noble Metals on the Nanoscale: Optical and Photothermal Properties and Some Applications in Imaging, Sensing, Biology, and Medicine. *Acc. Chem. Res.* **2008**, *41*, 1578– 1586.
19. El-Sayed, M. A. Some interesting properties of metals confined in time and nanometer space of different shapes. *Acc. Chem. Res*. **2001**, *34*, 257.
20. Bohren, C. F. How can a particle absorb more than the light incident on it? *Am. J. Phys*. **1983**, *51*, 323.
21. Linic, S.; Christopher, P.; Ingram, D. B. Plasmonic-metal nanostructures for efficient conversion of solar to chemical energy. *Nat. Mater*. **2011**, *10*, 911.
22. Langhammer, C.; Kasemo, B.; Zorić, I. Absorption and scattering of light by Pt, Pd, Ag, and Au nanodisks: absolute cross sections and branching ratios. *J. Chem. Phys*. **2007**, *126*, 194702.
23. Jain, P. K.; Lee, K. S.; El-Sayed, I. H.; El-Sayed, M. A.; Calculated Absorption and Scattering Properties of Gold Nanoparticles of Different Size, Shape, and Composition: Applications in Biological Imaging and Biomedicine. *J. Phys. Chem. B* **2006**, *110*, 7238.
24. Tan, C.; Chen, J.; Wu, X. J.; Zhang, H. Epitaxial Growth of Hybrid Nanostructures. *Nat. Rev. Mater.* **2018**, *3*, 17089
25. Li, M.; Luo, Z.; Zhao, Y. Self-Assembled Hybrid Nanostructures: Versatile Multifunctional Nanoplatforms for Cancer Diagnosis and Therapy. *Chem. Mater.* **2018**, *30*, 25– 53

26. Sangaiya, P.; Jayaprakash, R. A review on iron oxide nanoparticles and their biomedical applications. *J. Supercond. Novel Magn.* **2018**, *31*, 3397– 3413.
27. Wu, W.; Jiang, C.; Roy, V. A. L. Recent Progress in Magnetic Iron Oxide–Semiconductor Composite Nanomaterials as Promising Photocatalysts. *Nanoscale* **2015**, *7*, 38– 58.
28. Cortés, E.; Camargo, P. H. C. *Plasmonic catalysis from fundamentals to applications*; John Wiley & Sons, **2021**
29. Aditya, T.; Pal, A.; Pal, T. Nitroarene Reduction: A Trusted Model Reaction to Test Nanoparticle Catalysts. *Chem. Commun.* **2015**, *51*, 9410– 9431
30. Wunder, S.; Plzer, F.; Lu, Y.; Mei, Y.; Ballauff, M. Kinetic Analysis of Catalytic Reduction of 4-Nitrophenol by Metallic Nanoparticles Immobilized in Spherical Polyelectrolyte Brushes. *J. Phys. Chem. C* **2010**, *114*, 8814– 8820.
31. Hervés, V.; Pérez-Lorenzo, M.; Liz-Marzan, L. M.; Dzubiella, J.; Lu, Y.; Ballauff, M. Catalysis by Metallic Nanoparticles in Aqueous Solution: Model Reactions. *Chem. Soc. Rev.* **2012**, *41*, 5577– 5587
32. Brongersma, M. L.; Halas, N. J.; Nordlander, P. Plasmon-Induced Hot Carrier Science and Technology. *Nat. Nanotechnol.* **2015**, *10*, 25– 34
33. Devasia, D.; Das, A.; Mohan, V.; Jain, P. K. Control of Chemical Reaction Pathways by Light–Matter Coupling. *Annu. Rev. Phys. Chem.* **2021**, *72*, 423– 443.
34. De la Encarnación, C.; Lenzi, E.; Henriksen-Lacey, M.; Molina, B.; Jenkinson, K.; Herrero, A.; Colás, L.; Ramos-Cabrer, P.; Toro-Mendoza, J.; Orue, I.; Langer, J.; Bals, S.; Jimenez de Aberasturi, D.; Liz-Marzán, L. M. Hybrid Magnetic–Plasmonic Nanoparticle Probes for Multimodal Bioimaging. *J. Phys. Chem., C* **2022**, *126*, 19519– 19531
35. Rodrigues, M. P. D. S.; Dourado, A. H. B.; Cutolo, L. D. O.; Parreira, L. S.; Alves, T. V.; Slater, T. J. A.; Haigh, S. J.; Camargo, P. H. C.; de Torresi, S. I. C. Gold-Rhodium Nanoflowers for the Plasmon-Enhanced Hydrogen Evolution Reaction under Visible Light. *ACS Catal.* **2021**, *11*, 13543– 13555
36. Bastús, N. G.; Comenge, J.; Puntes, V. Kinetically Controlled Seeded Growth Synthesis of Citrate-Stabilized Gold Nanoparticles of up to 200 nm: Size Focusing Versus Ostwald Ripening. *Langmuir* **2011**, *27*, 11098– 11105

37. Haiss, W.; Thanh, N. T. K.; Aveyard, J.; Fernig, D. G. Determination of Size and Concentration of Gold Nanoparticles from UV-Vis Spectra. *Anal. Chem.* **2007**, *79*, 4215– 4221
38. Roy, S.; Rao, A.; Devatha, G.; Pillai, P. P. Revealing the Role of Electrostatics in Gold-Nanoparticle-Catalyzed Reduction of Charged Substrates. *ACS Catal.* **2017**, *7*, 7141– 7145.
39. Roy, S.; Roy, S.; Rao, A.; Devatha, G.; Pillai, P. P. Precise Nanoparticle–Reactant Interaction Outplays Ligand Poisoning in Visible-Light Photocatalysis. *Chem. Mater.* **2018**, *30*, 8415– 8419
40. Gavilán, H.; Sánchez, E. H.; Brollo, M. E. F.; Asín, L.; Moerner, K. K.; Frandsen, C.; Lázaro, F. J.; Serna, C. J.; Veintemillas-Verdaguer, S.; Morales, M. P.; Gutiérrez, L. Formation Mechanism of Maghemite Nanoflowers Synthesized by a Polyol-Mediated Process. *ACS Omega* **2017**, *2*, 7172– 7184
41. Skrabalak, S. E.; Wiley, B. J.; Kim, M.; Formo, E. V.; Xia, Y. On the polyol synthesis of silver nanostructures: glycolaldehyde as a reducing agent. *Nano Lett.* **2008**, *8*, 2077– 2081.
42. Ai, Q.; Yuan, Z.; Huang, R.; Yang, C.; Jiang, G.; Xiong, J.; Huang, Z.; Yuan, S. One-Pot Co-Precipitation Synthesis of Fe_3O_4 Nanoparticles Embedded in 3D Carbonaceous Matrix as Anode for Lithium Ion Batteries. *J. Mater. Sci.* **2019**, *54*, 4212– 4224
43. Kim, Y.; Wilson, A. J.; Jain, P. K. The nature of plasmonically assisted hot-electron transfer in a donor–bridge–acceptor complex. *ACS Catal.* **2017**, *7*, 4360– 4365
44. Kim, Y.; Smith, J. G.; Jain, P. K. Harvesting Multiple Electron–Hole Pairs Generated Through Plasmonic Excitation of Au Nanoparticles. *Nat. Chem.* **2018**, *10*, 763– 769
45. Kim, Y.; Dumett Torres, D.; Jain, P. K. Activation Energies of Plasmonic Catalysts. *Nano Lett.* **2016**, *16*, 3399– 3407

JOHN WILEY AND SONS LICENSE
TERMS AND CONDITIONS

Jan 26, 2024

This Agreement between Ms. Angela Kadlas ("You") and John Wiley and Sons ("John Wiley and Sons") consists of your license details and the terms and conditions provided by John Wiley and Sons and Copyright Clearance Center.

License Number	5716470033081
License date	Jan 26, 2024
Licensed Content Publisher	John Wiley and Sons
Licensed Content Publication	Wiley Books
Licensed Content Title	Theory of Plasmonic Excitations
Licensed Content Author	Alexander O. Govorov, Zhiming M. Wang, Xiang-Tian Kong, et al
Licensed Content Date	Jun 11, 2021
Licensed Content Pages	35
Type of use	Dissertation/Thesis
Requestor type	University/Academic
Format	Print and electronic
Portion	Figure/table
Number of figures/tables	1
Will you be translating?	No

Title of new work	Multi-Functional Fe3O4-Au Hybrid Nanostructures for Catalytic Studies
Institution name	Indian Institute of Science Education and Research Pune
Expected presentation date	May 2024
Order reference number	1
Portions	figure 1.2
Requestor Location	Ms. Angela Kadlas Department of Chemistry IISER Pune Pune, 411008 India Attn: Ms. Angela Kadlas
Publisher Tax ID	EU826007151
Total	0.00 USD

Terms and Conditions

TERMS AND CONDITIONS

This copyrighted material is owned by or exclusively licensed to John Wiley & Sons, Inc. or one of its group companies (each a"Wiley Company") or handled on behalf of a society with which a Wiley Company has exclusive publishing rights in relation to a particular work (collectively "WILEY"). By clicking "accept" in connection with completing this licensing transaction, you agree that the following terms and conditions apply to this transaction (along with the billing and payment terms and conditions established by the Copyright Clearance Center Inc., ("CCC's Billing and Payment terms and conditions"), at the time that you opened your RightsLink account (these are available at any time at http://myaccount.copyright.com).

Terms and Conditions

- The materials you have requested permission to reproduce or reuse (the "Wiley Materials") are protected by copyright.
- You are hereby granted a personal, non-exclusive, non-sub licensable (on a stand-alone basis), non-transferable, worldwide, limited license to reproduce the Wiley Materials for the purpose specified in the licensing process. This license, **and any CONTENT (PDF or image file) purchased as part of your order,** is for a one-time use only and limited to any maximum distribution number specified in the

license. The first instance of republication or reuse granted by this license must be completed within two years of the date of the grant of this license (although copies prepared before the end date may be distributed thereafter). The Wiley Materials shall not be used in any other manner or for any other purpose, beyond what is granted in the license. Permission is granted subject to an appropriate acknowledgement given to the author, title of the material/book/journal and the publisher. You shall also duplicate the copyright notice that appears in the Wiley publication in your use of the Wiley Material. Permission is also granted on the understanding that nowhere in the text is a previously published source acknowledged for all or part of this Wiley Material. Any third party content is expressly excluded from this permission.

- With respect to the Wiley Materials, all rights are reserved. Except as expressly granted by the terms of the license, no part of the Wiley Materials may be copied, modified, adapted (except for minor reformatting required by the new Publication), translated, reproduced, transferred or distributed, in any form or by any means, and no derivative works may be made based on the Wiley Materials without the prior permission of the respective copyright owner.**For STM Signatory Publishers clearing permission under the terms of the STM Permissions Guidelines only, the terms of the license are extended to include subsequent editions and for editions in other languages, provided such editions are for the work as a whole in situ and does not involve the separate exploitation of the permitted figures or extracts,** You may not alter, remove or suppress in any manner any copyright, trademark or other notices displayed by the Wiley Materials. You may not license, rent, sell, loan, lease, pledge, offer as security, transfer or assign the Wiley Materials on a stand-alone basis, or any of the rights granted to you hereunder to any other person.

- The Wiley Materials and all of the intellectual property rights therein shall at all times remain the exclusive property of John Wiley & Sons Inc, the Wiley Companies, or their respective licensors, and your interest therein is only that of having possession of and the right to reproduce the Wiley Materials pursuant to Section 2 herein during the continuance of this Agreement. You agree that you own no right, title or interest in or to the Wiley Materials or any of the intellectual property rights therein. You shall have no rights hereunder other than the license as provided for above in Section 2. No right, license or interest to any trademark, trade name, service mark or other branding ("Marks") of WILEY or its licensors is granted hereunder, and you agree that you shall not assert any such right, license or interest with respect thereto

- NEITHER WILEY NOR ITS LICENSORS MAKES ANY WARRANTY OR REPRESENTATION OF ANY KIND TO YOU OR ANY THIRD PARTY, EXPRESS, IMPLIED OR STATUTORY, WITH RESPECT TO THE MATERIALS OR THE ACCURACY OF ANY INFORMATION CONTAINED IN THE MATERIALS, INCLUDING, WITHOUT LIMITATION, ANY IMPLIED WARRANTY OF MERCHANTABILITY, ACCURACY, SATISFACTORY QUALITY, FITNESS FOR A PARTICULAR PURPOSE, USABILITY, INTEGRATION OR NON-INFRINGEMENT AND ALL SUCH WARRANTIES ARE HEREBY EXCLUDED BY WILEY AND ITS LICENSORS AND WAIVED BY YOU.

- WILEY shall have the right to terminate this Agreement immediately upon breach of this Agreement by you.

- You shall indemnify, defend and hold harmless WILEY, its Licensors and their respective directors, officers, agents and employees, from and against any actual or threatened claims, demands, causes of action or proceedings arising from any

breach of this Agreement by you.

- IN NO EVENT SHALL WILEY OR ITS LICENSORS BE LIABLE TO YOU OR ANY OTHER PARTY OR ANY OTHER PERSON OR ENTITY FOR ANY SPECIAL, CONSEQUENTIAL, INCIDENTAL, INDIRECT, EXEMPLARY OR PUNITIVE DAMAGES, HOWEVER CAUSED, ARISING OUT OF OR IN CONNECTION WITH THE DOWNLOADING, PROVISIONING, VIEWING OR USE OF THE MATERIALS REGARDLESS OF THE FORM OF ACTION, WHETHER FOR BREACH OF CONTRACT, BREACH OF WARRANTY, TORT, NEGLIGENCE, INFRINGEMENT OR OTHERWISE (INCLUDING, WITHOUT LIMITATION, DAMAGES BASED ON LOSS OF PROFITS, DATA, FILES, USE, BUSINESS OPPORTUNITY OR CLAIMS OF THIRD PARTIES), AND WHETHER OR NOT THE PARTY HAS BEEN ADVISED OF THE POSSIBILITY OF SUCH DAMAGES. THIS LIMITATION SHALL APPLY NOTWITHSTANDING ANY FAILURE OF ESSENTIAL PURPOSE OF ANY LIMITED REMEDY PROVIDED HEREIN.

- Should any provision of this Agreement be held by a court of competent jurisdiction to be illegal, invalid, or unenforceable, that provision shall be deemed amended to achieve as nearly as possible the same economic effect as the original provision, and the legality, validity and enforceability of the remaining provisions of this Agreement shall not be affected or impaired thereby.

- The failure of either party to enforce any term or condition of this Agreement shall not constitute a waiver of either party's right to enforce each and every term and condition of this Agreement. No breach under this agreement shall be deemed waived or excused by either party unless such waiver or consent is in writing signed by the party granting such waiver or consent. The waiver by or consent of a party to a breach of any provision of this Agreement shall not operate or be construed as a waiver of or consent to any other or subsequent breach by such other party.

- This Agreement may not be assigned (including by operation of law or otherwise) by you without WILEY's prior written consent.

- Any fee required for this permission shall be non-refundable after thirty (30) days from receipt by the CCC.

- These terms and conditions together with CCC's Billing and Payment terms and conditions (which are incorporated herein) form the entire agreement between you and WILEY concerning this licensing transaction and (in the absence of fraud) supersedes all prior agreements and representations of the parties, oral or written. This Agreement may not be amended except in writing signed by both parties. This Agreement shall be binding upon and inure to the benefit of the parties' successors, legal representatives, and authorized assigns.

- In the event of any conflict between your obligations established by these terms and conditions and those established by CCC's Billing and Payment terms and conditions, these terms and conditions shall prevail.

- WILEY expressly reserves all rights not specifically granted in the combination of (i) the license details provided by you and accepted in the course of this licensing transaction, (ii) these terms and conditions and (iii) CCC's Billing and Payment terms and conditions.

- This Agreement will be void if the Type of Use, Format, Circulation, or Requestor Type was misrepresented during the licensing process.

- This Agreement shall be governed by and construed in accordance with the laws of the State of New York, USA, without regards to such state's conflict of law rules. Any legal action, suit or proceeding arising out of or relating to these Terms and Conditions or the breach thereof shall be instituted in a court of competent jurisdiction in New York County in the State of New York in the United States of America and each party hereby consents and submits to the personal jurisdiction of such court, waives any objection to venue in such court and consents to service of process by registered or certified mail, return receipt requested, at the last known address of such party.

WILEY OPEN ACCESS TERMS AND CONDITIONS

Wiley Publishes Open Access Articles in fully Open Access Journals and in Subscription journals offering Online Open. Although most of the fully Open Access journals publish open access articles under the terms of the Creative Commons Attribution (CC BY) License only, the subscription journals and a few of the Open Access Journals offer a choice of Creative Commons Licenses. The license type is clearly identified on the article.

The Creative Commons Attribution License

The Creative Commons Attribution License (CC-BY) allows users to copy, distribute and transmit an article, adapt the article and make commercial use of the article. The CC-BY license permits commercial and non-

Creative Commons Attribution Non-Commercial License

The Creative Commons Attribution Non-Commercial (CC-BY-NC)License permits use, distribution and reproduction in any medium, provided the original work is properly cited and is not used for commercial purposes.(see below)

Creative Commons Attribution-Non-Commercial-NoDerivs License

The Creative Commons Attribution Non-Commercial-NoDerivs License (CC-BY-NC-ND) permits use, distribution and reproduction in any medium, provided the original work is properly cited, is not used for commercial purposes and no modifications or adaptations are made. (see below)

Use by commercial "for-profit" organizations

Use of Wiley Open Access articles for commercial, promotional, or marketing purposes requires further explicit permission from Wiley and will be subject to a fee.

Further details can be found on Wiley Online Library
http://olabout.wiley.com/WileyCDA/Section/id-410895.html

Other Terms and Conditions:

v1.10 Last updated September 2015

Questions? customercare@copyright.com.

Marketplace

Order Confirmation

Thank you, your order has been placed. An email confirmation has been sent to you. Your order license details and printable licenses will be available within 24 hours. Please access Manage Account for final order details.

This is not an invoice. Please go to manage account to access your order history and invoices.

CUSTOMER INFORMATION

Payment by invoice: You can cancel your order until the invoice is generated by contacting customer service.

Billing Address

Ms. Angela Kadlas
Department of Chemistry
IISER Pune
Pune, 411008
India

+91 7875736504
angela.kadlas@students.iiserpune.ac.in

Customer Location

Ms. Angela Kadlas
Department of Chemistry
IISER Pune
Pune, 411008
India

PO Number (optional)

N/A

Payment options

Invoice

PENDING ORDER CONFIRMATION

Confirmation Number: Pending

Order Date: 26-Jan-2024

1. Chemical Society reviews

0.00 USD

Article: Catalysis by metallic nanoparticles in aqueous solution: model reactions.

Order License ID	Pending	**Publisher**	ROYAL SOCIETY OF CHEMISTRY
ISSN	1460-4744		
Type of Use	Republish in a thesis/dissertation	**Portion**	Chart/graph/table/figure

LICENSED CONTENT

Publication Title	Chemical Society reviews	**Publication Type**	e-Journal
Article Title	Catalysis by metallic nanoparticles in aqueous solution: model reactions.	**Start Page**	5577
		End Page	5587
Author/Editor	Royal Society of Chemistry (Great Britain)	**Issue**	17
		Volume	41
Date	01/01/1972	**URL**	http://www.rsc.org/csr
Language	English		
Country	United Kingdom of Great Britain and Northern Ireland		
Rightsholder	Royal Society of Chemistry		

REQUEST DETAILS

Portion Type	Chart/graph/table/figure	**Distribution**	Worldwide

Number of Charts / Graphs / Tables / Figures Requested	1	Translation	Original language of publication
Format (select all that apply)	Print, Electronic	Copies for the Disabled?	No
Who Will Republish the Content?	Academic institution	Minor Editing Privileges?	No
Duration of Use	Life of current edition	Incidental Promotional Use?	No
Lifetime Unit Quantity	Up to 499	Currency	USD
Rights Requested	Main product		

NEW WORK DETAILS

Title	Multi-Functional Fe3O4-Au Hybrid Nanostructures for Catalytic Studies	Institution Name	Indian Institute of Science Education and Research Pune, India
Instructor Name	Dr. Pramod Pillai	Expected Presentation Date	2024-05-11

ADDITIONAL DETAILS

Order Reference Number	N/A	The Requesting Person / Organization to Appear on the License	Angela Kadlas

REQUESTED CONTENT DETAILS

Title, Description or Numeric Reference of the Portion(s)	Figure 2	Title of the Article / Chapter the Portion Is From	Catalysis by metallic nanoparticles in aqueous solution: model reactions.
Editor of Portion(s)	Hervés, Pablo; Pérez-Lorenzo, Moisés; Liz-Marzán, Luis M.; Dzubiella, Joachim; Lu, Yan; Ballauff, Matthias	Author of Portion(s)	Hervés, Pablo; Pérez-Lorenzo, Moisés; Liz-Marzán, Luis M.; Dzubiella, Joachim; Lu, Yan; Ballauff, Matthias
Volume / Edition	41 / ONLINE		
Page or Page Range of Portion	5577-5587	Issue, if Republishing an Article From a Serial	17
		Publication Date of Portion	2012-09-07

Total Items: 1

Total Due: 0.00 USD

Accepted: Marketplace Permissions General Terms and Conditions and any applicable Publisher Terms and Conditions